

Supporting information

Mechanistic study of photocatalytic CO₂ reduction using a Ru(II)-Re(I) supramolecular photocatalyst

Kei Kamogawa,^a Yushi Shimoda,^b Kiyoshi Miyata,^b Ken Onda,^{*b} Yasuomi Yamazaki,^c Yusuke Tamaki,^a Osamu Ishitani^{*a}

^aDepartment of Chemistry, Tokyo Institute of Technology, O-okayama 2-12-1, NE1, Meguro-ku, Tokyo 152-8550, Japan. E-mail: ishitani@chem.titech.ac.jp

^bDepartment of Chemistry, Kyushu University, Fukuoka 819-0395, Japan. E-mail: konda@chem.kyushu-univ.jp

^cDepartment of Materials and Life Science, Graduate School of Science and Engineering, Seikei University, 3-3-1 Kichijoji-kitamachi, Musashino-shi, Tokyo 180-8633, Japan.

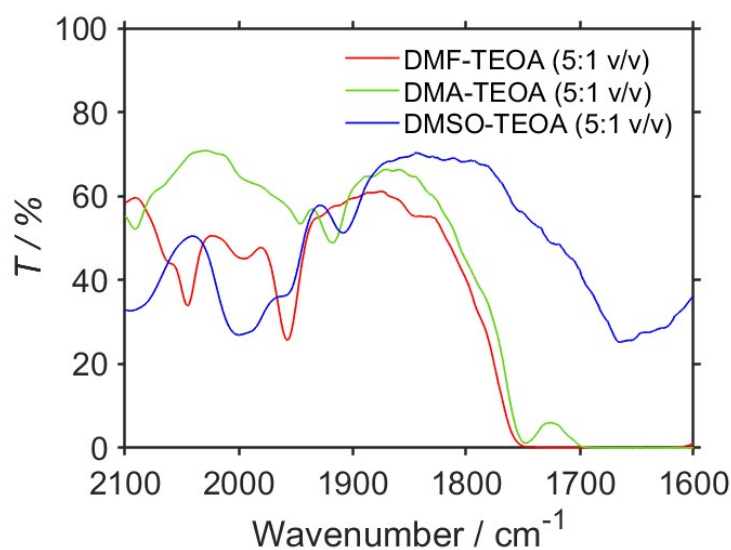


Fig. S1 FT-IR spectra of the DMF-TEOA (5:1 v/v) (red), DMA-TEOA (5:1 v/v) (green), and DMSO-TEOA (5:1 v/v) (blue) sample solutions; d = 0.2 mm.

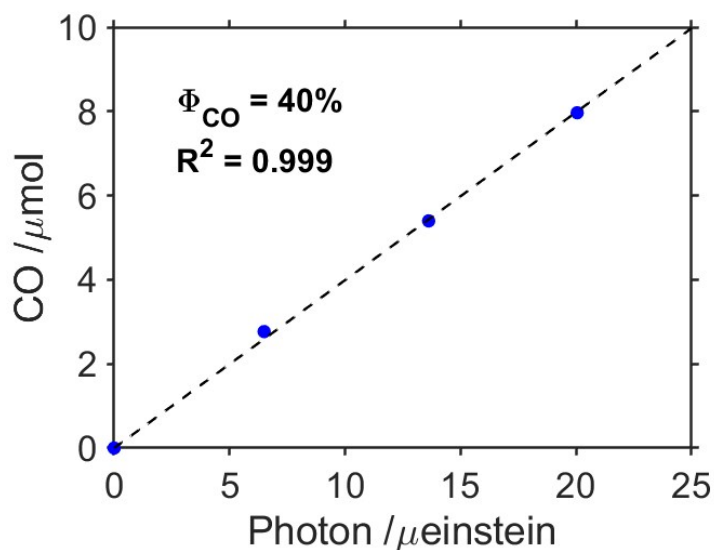


Fig. S2 Dependence of the formation of CO on the amount of photons absorbed over irradiation times of 30, 60, and 90 min. A CO₂-saturated DMSO–TEOA (5:1 v/v) solution containing **RuC2Re** (0.05 mM) and BIH (0.1 M) was irradiated at $\lambda_{\text{ex}} = 480$ nm (light intensity: 5.0×10^{-9} einstein s⁻¹).

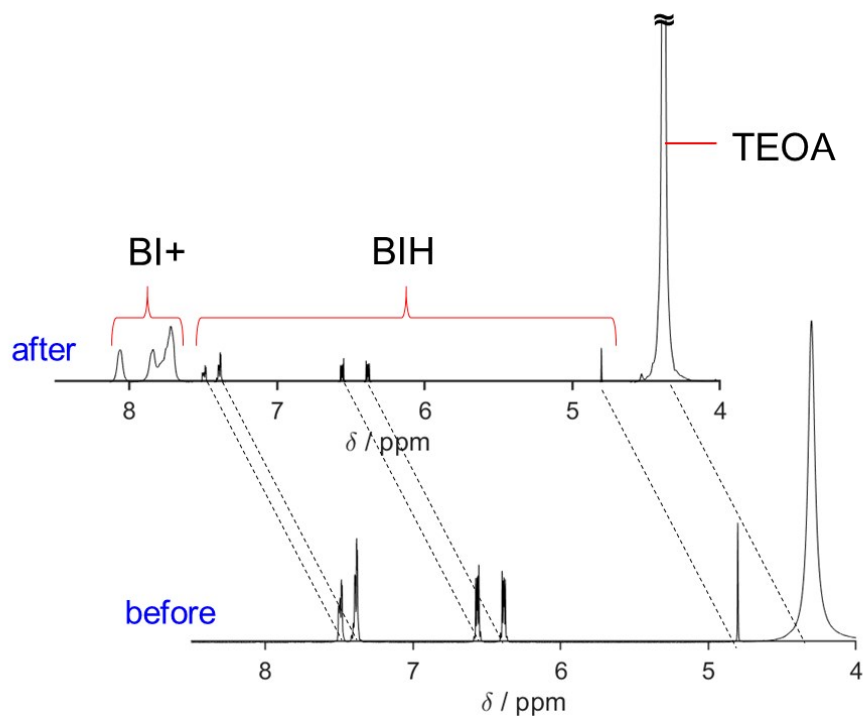


Fig. S3 ¹H NMR spectra of the reaction solutions before and after 22 h of irradiation; DMSO-d₆ containing TEOA (1.26 M), BIH (0.1 M), **RuC2Re** (0.14 mM), and ¹³CO₂ (537 Torr) was irradiated at 490–620 nm ($\lambda_{\text{max}} = 530$ nm) using an LED lamp.

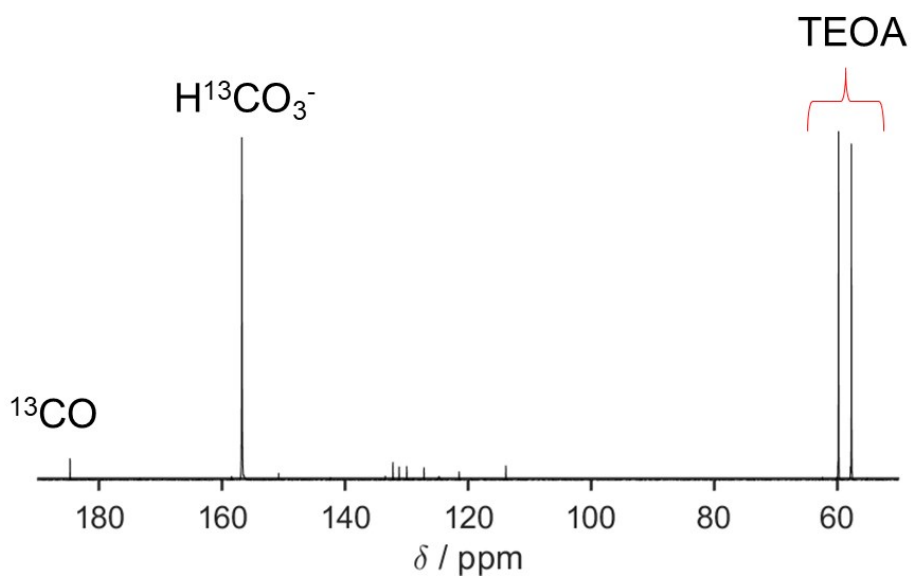


Fig. S4 ^{13}C NMR spectra of the reaction solution after 22 h of irradiation (NOE complete ^1H -decoupling method); DMSO- d_6 containing TEOA (1.26 M), BIH (0.1 M), **RuC2Re** (0.14 mM), and $^{13}\text{CO}_2$ (537 Torr) was irradiated at 490–620 nm ($\lambda_{\text{max}} = 530$ nm) using an LED lamp.

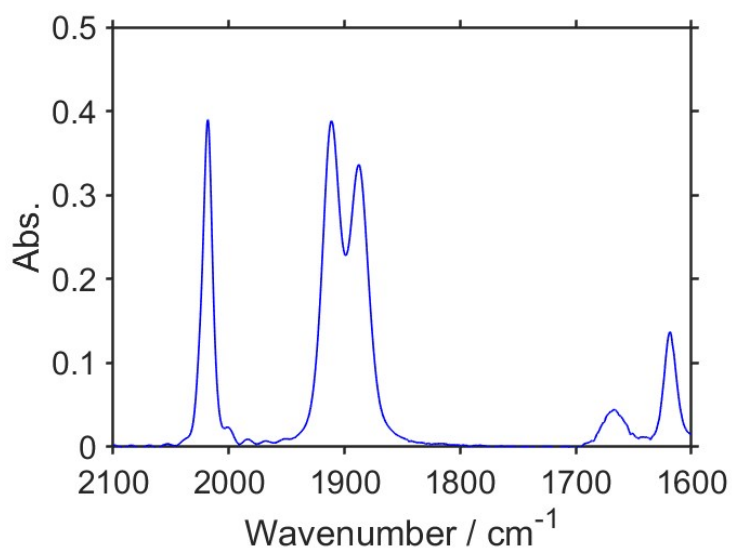


Fig. S5 FT-IR spectrum of **RuC2Re** (6 mM) in DMSO-TEOA (5:1 v/v); $d = 0.2$ mm.

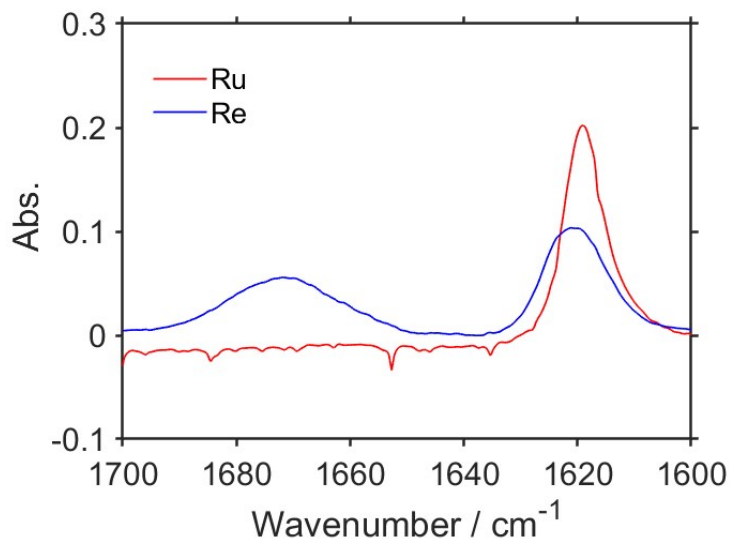


Fig. S6 FT-IR spectrum of **Ru** (red, 5 mM) and **Re** (blue, 5 mM) measured in DMSO–THF–TEOA (5:5:2 v/v); $d = 0.5$ mm.

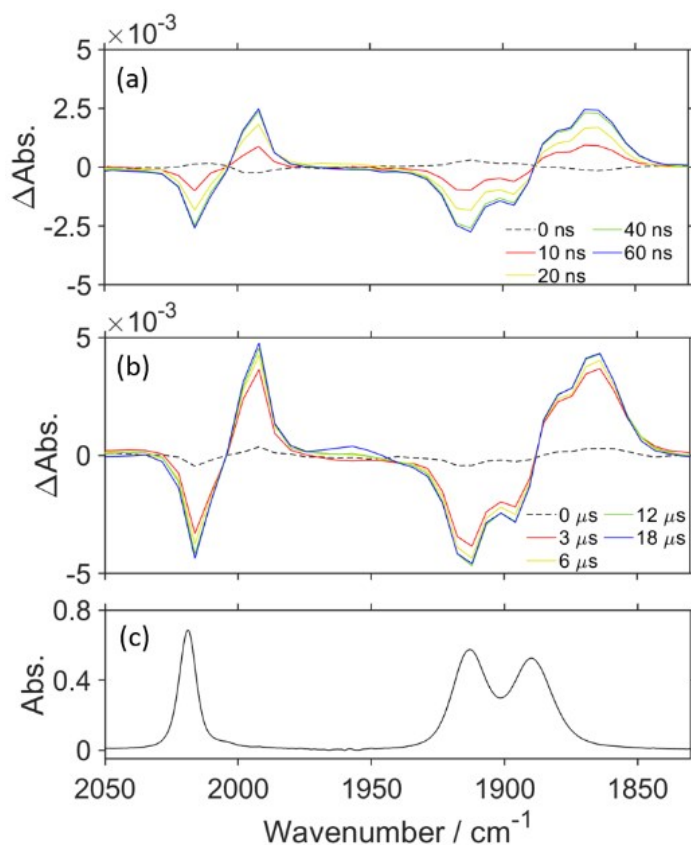


Fig. S7 TR-IR spectra measured at the indicated time delay after pulsed 532 nm excitation, (a) up to 60 ns and (b) up to 18 μ s. A DMSO–THF–TEOA (5:5:2 v/v) solution containing **RuC2Re** (1.0 mM) and BIH (0.1 M) was irradiated using 532 nm pump light (50 Hz) and probed (100 Hz). (c) FT-IR spectrum of **RuC2Re** (3 mM) in DMSO–THF–TEOA (5:5:2 v/v); $d = 0.5$ mm.

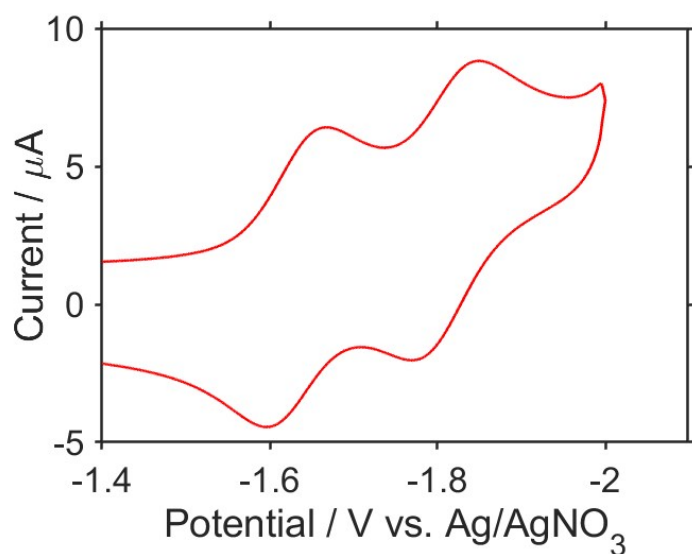


Fig. S8 CV of **Ru** in a DMSO-TEOA (5:1 v/v) solution under an Ar atmosphere; WE: glassy carbon (diameter = 3 mm), RE: 0.01 mM Ag/AgNO₃, CE: Pt wire, supporting electrolyte: Et₄NBF₄ (0.1 M), scan rate: 200 mV s⁻¹.

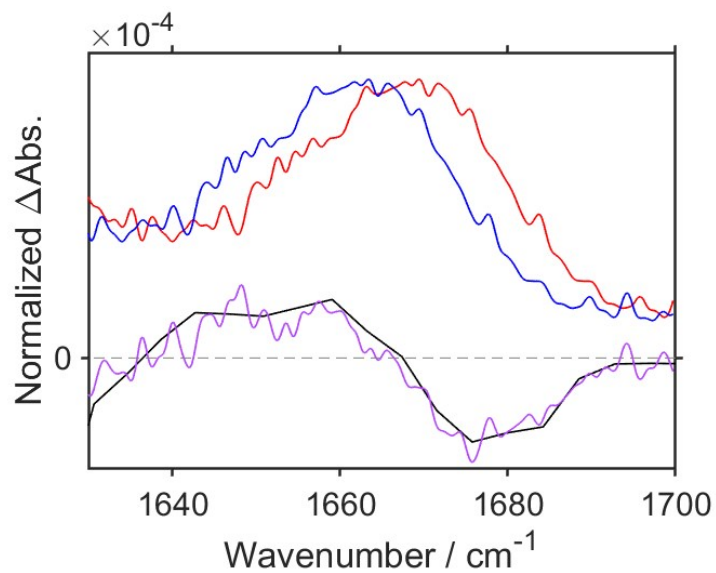


Fig. S9 TR-IR spectrum at 50 ns after excitation (black line, Figure 5a) and the difference FT-IR spectrum (purple) between the spectrum of **RuC₂Re** (red) and its low-wavenumber (6 cm⁻¹) shifted spectrum (blue).

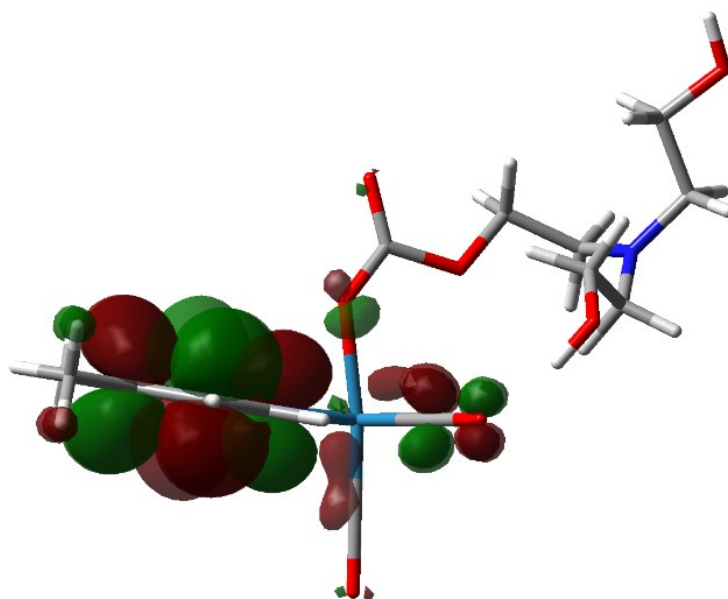


Fig. S10 Charge distribution of the SOMO of Re^- obtained from DFT calculations using the M06 functional and LanL2DZ basis set.

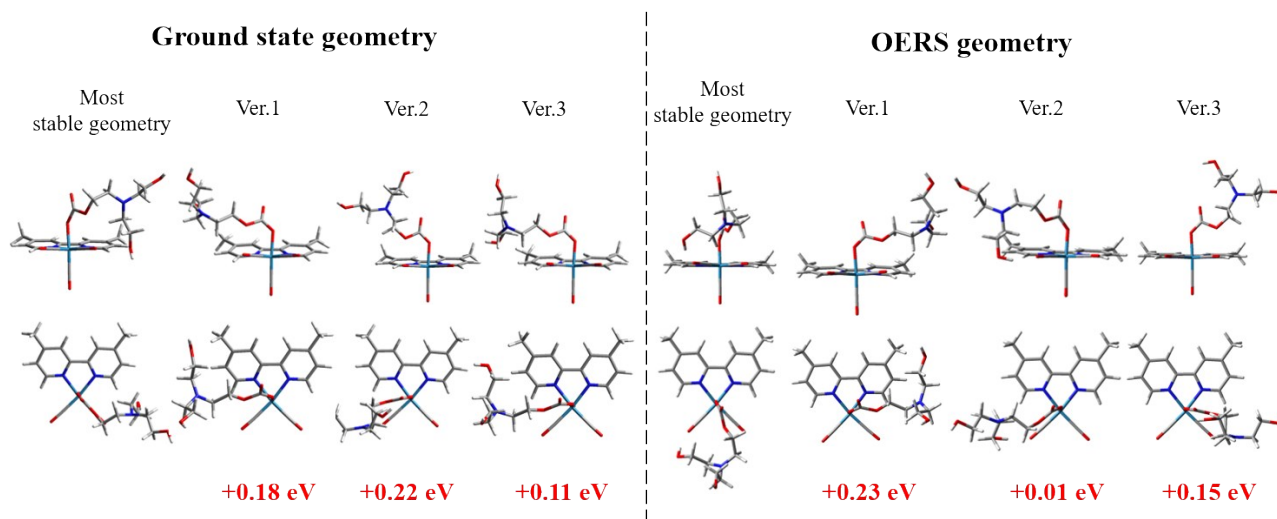


Fig. S11 Stable structure of Re and Re^- (red letters indicate the energy difference from the most stable structure).

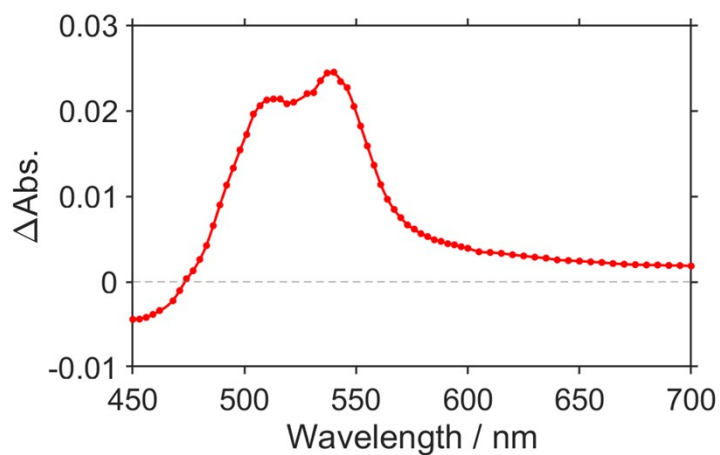


Fig. S12 TR-vis absorption spectrum of **Ru** (0.2 mM) in a CO₂ saturated DMSO–TEOA (5:1 v/v) solution containing BIH (0.1 M) measured at 800 μs after 532 nm excitation.

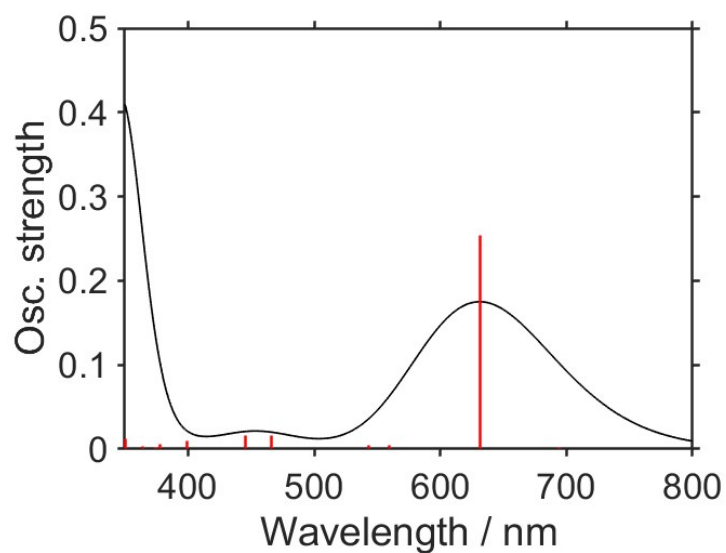


Fig. S13 Oscillator strengths of BI• obtained from the TDDFT calculation of the optimised structure using DFT in dimethyl sulfoxide (PCM) with a UB3LYP exchange correlation functional and the 6-311G++(d,p) basis set (red line), and its UV-vis absorption spectra estimated by the summation of the Gaussian functions on the basis of the oscillation strengths (black line).

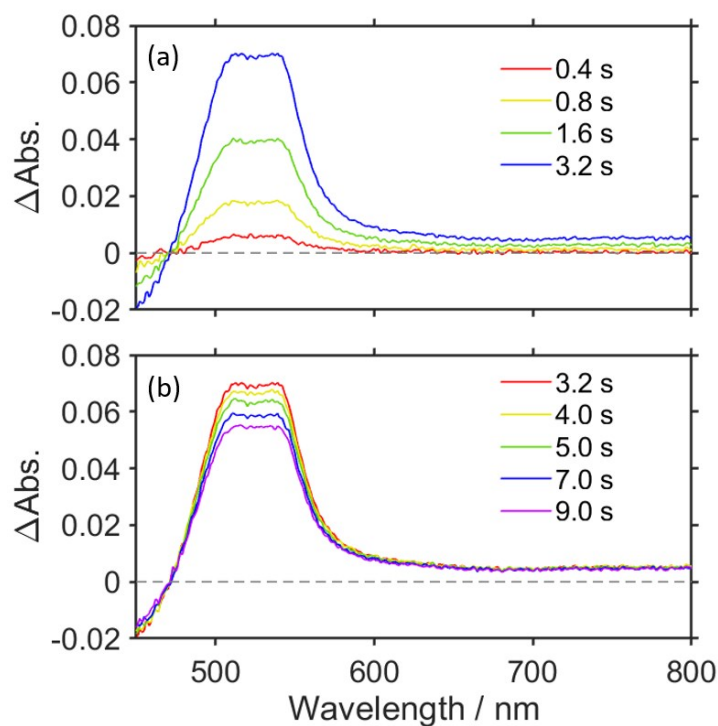


Fig. S14 (a) UV-vis differential absorption spectra of **Ru** (0.05 mM) in Ar-saturated DMSO-TEOA (5:1 v/v) solution containing BIH (0.1 M) during irradiation. (b) UV-vis differential absorption spectra of **Ru** (0.05 mM) in Ar-saturated DMSO-TEOA (5:1 v/v) solution containing BIH (0.1 M) after irradiation; $I_{\text{ex}} = 480 \text{ nm}$ ($5.3 \times 10^{-9} \text{ einstein s}^{-1}$).

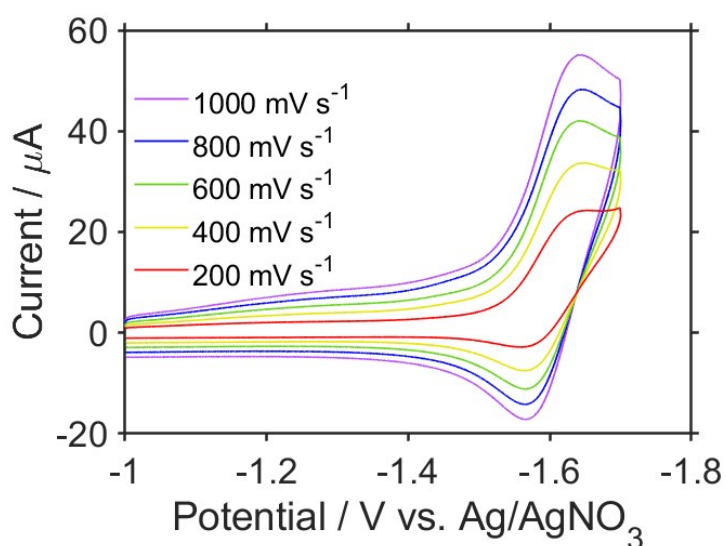


Fig. S15 CV showing the dependence of the scan rate of **Re** (2 mM) over a scan rate range of 200–1000 mV s^{-1} at $T = 298 \text{ K}$.

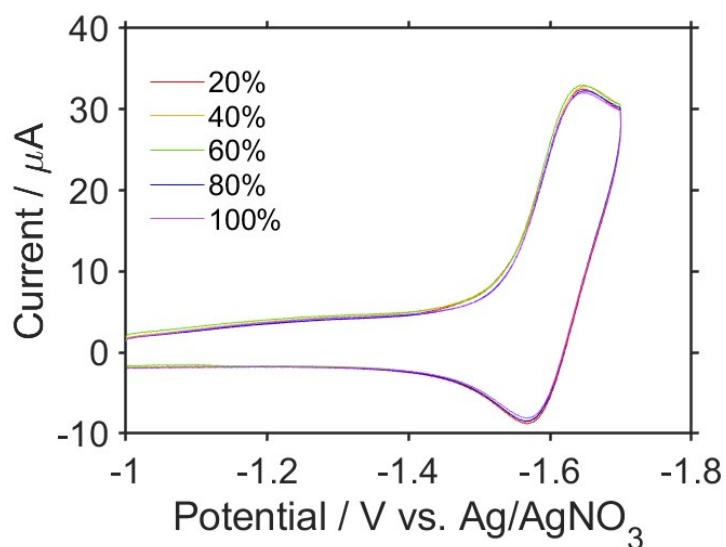


Fig. S16 CVs of **Re** in a DMSO-TEOA solution purged with CO_2 ($x\%$) and Ar ($100 - x\%$) ($x = 20, 40, 60, 80,$ and 100); WE: glassy carbon electrode (diameter = 3 mm), RE: 0.01 mM Ag/AgNO₃, CE: Pt wire, supporting electrolyte: Et₄NBF₄ (0.1 M), scan rate: 400 mV s⁻¹.

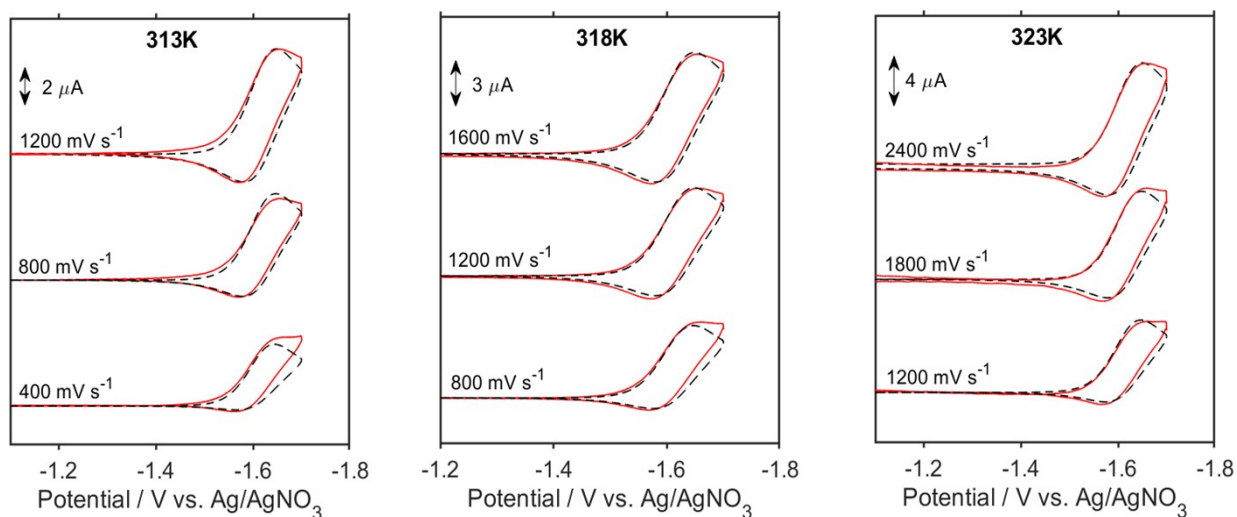


Fig. S17 Background subtracted CVs (red) of **Re** (2 mM) and simulated CVs (black). The fitting parameters and experimental conditions were as follows: $E_1 = -1.61$ V ($k_s = 0.1$ cm s⁻¹), $k_c = 4.9$ (313 K), 6.0 (318 K), 9.6 (323 K) s⁻¹, $D = 1.32 \times 10^{-6}$ cm² s⁻¹; WE: glassy carbon (diameter = 1 mm), RE: 0.01 mM Ag/AgNO₃, CE: Pt wire, supporting electrolyte: 0.1 M Et₄NBF₄ (0.1 M): $k_c = 4.9$ s⁻¹ at 313 K, 6.0 s⁻¹ at 318 K, and 9.6 s⁻¹ at 323 K.

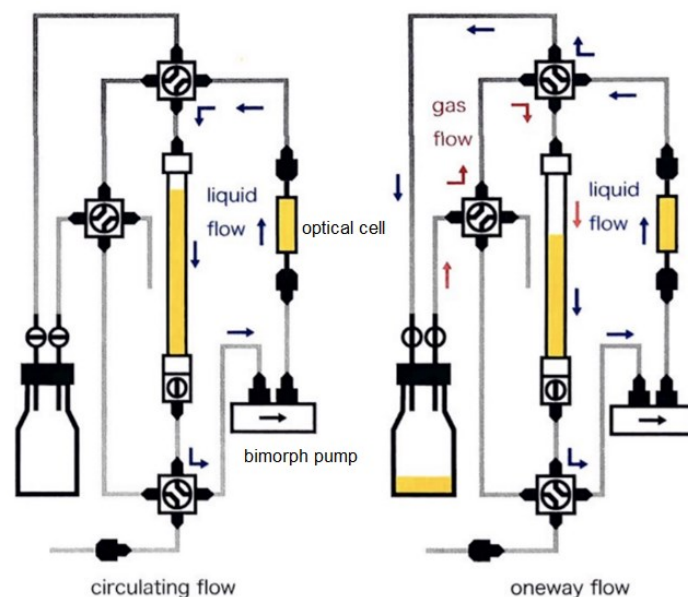


Fig. S18 Flow cell systems used in the TR spectroscopic measurements.

Table S1 Electron density for each unit from the Mulliken analysis of the most stable nonreduced state (S_0) and the OERS of Re.

	Mulliken Charge							
	Re	CO ¹⁾	CO ²⁾	CO ³⁾	dmb	-OC(O)O-	-CH ₂ CH ₂ NR ₂	Total
S_0	0.859	-0.203	-0.171	-0.247	0.318	-0.812	0.256	0.000
OERS	0.921	-0.239	-0.308	-0.284	-0.444	-0.813	0.168	-1.000
OERS-S_0	0.062	-0.036	-0.138	-0.037	-0.762	-0.001	-0.088	-1.000

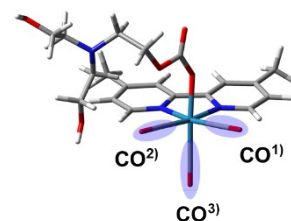


Table S2 Electron density for each unit from the Mulliken analysis of the stable nonreduced state (S_0) and the OERS of Re.

	Mulliken charge																
	S_0	Re	CO	dmb	CO ₂	TEOA	Total	OERS	Re	CO	dmb	CO ₂	TEOA	Total			
ver1	0.86	-0.17	-0.20	-0.24	0.29	-0.80	0.25	0.00	ver1	0.88	-0.24	-0.27	-0.29	-0.48	-0.81	0.20	-1.00
ver2	0.86	-0.16	-0.20	-0.24	0.32	-0.82	0.24	0.00	ver2	0.89	-0.25	-0.27	-0.27	-0.44	-0.81	0.16	-1.00
ver3	0.86	-0.17	-0.20	-0.24	0.30	-0.81	0.25	0.00	ver3	0.88	-0.23	-0.27	-0.29	-0.46	-0.82	0.19	-1.00